The Role of Interphase on Micro- to Macroscopic Responses and Prediction for Initiation of Debonding Damage of Glass-Fiber Reinforced Polycarbonate

N. Esmaeili, Y. Tomita

The Role of Interphase on Micro- to Macroscopic Responses and Prediction for Initiation of Debonding Damage of Glass–Fiber Reinforced Polycarbonate

N. ESMAEILI* AND Y. TOMITA

Graduate School of Science and Technology, Kobe University
1-1, Rokkodai-cho, Nada Kobe, Japan 657-8501

ABSTRACT: A computational model based on large-deformation finite element method (FEM) analysis is developed and used to evaluate the interaction between the microstructure and the heterogeneous deformation behavior of ternary composites on micro- to macroscopic scales. To uncover the influence of the plastic interphase layer on the stress–strain behavior of the three-phase system under constant strain-rate loading, the analyses of two different types of polymers with different Poisson's ratios are performed. In particular, we investigate the effects of the interphase on the normal stress at the fiber surface to predict the initiation of glass fiber–polymer matrix debonding damage. An interphase with stiffness well below that of the matrix shows a suitable effect on the micro- to macroscopic deformation behavior and suppresses the initiation of debonding, while an interphase Poisson's ratio between that of the fiber and the matrix is preferable. Furthermore, computational simulation has been performed to clarify the effects of the interphase thickness and fiber volume fraction on the normal stress at the fiber surface. The results obtained using the models suggest the realization of favorable interphase properties for suppressing the initiation of debonding at the fiber surface and improving the functionality of the reinforced polymer.

KEY WORDS: computational simulation, polymer-based reinforced composite debonding, interphase layer, shear band, stress distribution.

*Author to whom correspondence should be addressed. E-mail: oesmaeili@gmail.com
Figures 1–3, 5, 7 and 8 appear in color online: http://ijd.sagepub.com

1056-7895/08/01 0045–20 $10.00/0 DOI: 10.1177/1056789506067936

Los Angeles, London, New Delhi and Singapore

INTRODUCTION

INTERPHASES PLAY A key role in all multicomponent materials irrespective of the number and type of components or their actual structure. They are equally important in particulate-filled polymer, polymer blends, fiber-reinforced advanced composites, nanocomposites, and biomimetic materials. Recognition of the role of the main factors that influence interfacial adhesion and proper surface modification may lead to significant progress in many fields of research and development, as well as in related technologies. The basic condition of the application of fiber-reinforced composites is perfect adhesion between the components. Perfect adhesion is essential to transfer load from the matrix to the fiber. Without perfect adhesion, the principle of fiber-reinforced systems, i.e., the strong fibers carry the load, while the matrix distributes it and transfers it from one fiber to the other, would be invalid.

The importance of interphases is recognized by all those who are involved in the study of heterogeneous multiphase materials. In some cases, interfacial interactions are claimed to govern the properties of composites (Eirich, 1984; Kardos, 1985). However, there are few publications available on studies in which the large deformation in blended polymer materials in the presence of an interphase layer has been taken into account. The study of a coated particle embedded within a matrix under a multiaxial load, has revealed that the elasticity modulus of the interphase must be smaller than that of the matrix to reduce the stress concentration in the matrix (Lauke et al., 2000). The elastic properties of sphere-reinforced composites have been investigated by considering the mesophase between a particle and a matrix, and it has been found that an appropriately designed interphase significantly improves the strength and toughness of composites (Mai et al., 1998; Llorca et al., 2000).

In particulate-filled polymers, the assumption of an interlayer with varying properties may explain the strong dependence of yield stress and strength on particle size (Pukánszky, 1990). An improved model, including plasticity, for the prediction of the stress in fibers with an interface/interphase region, clarified that, quite often, the appropriate size of the fibers provides an interphase with a modulus slightly lower than that of the matrix, thereby improving the reliability of the composites (Johnson et al., 2005). The mechanical behavior of a particulate biocomposite with an elasto-plastic matrix has been found to be markedly influenced by interfacial adhesion, which is characterized using the different

strengths of the interphase region (Fan et al., 2004). The application of an elastomeric interlayer was also suggested to decrease stress concentration around the fibers (Kardos, 1985). Interfacial debonding around the interphase region was considered in the formulation of a model by the vanishing finite element technique (Li et al., 2000). Several studies have been made on the large deformation behavior of two-phase blended polymers. Among them, computational simulations employing realistic constitutive equations of polymers have been performed (Arruda and Boyce, 1993; Tomita and Tanaka, 1995; Tanaka et al., 2000; Pijnenburg and Van der Giessen, 2001; Tomita and Lu, 2002). In the case of particle-reinforced glassy polymers, it has been pointed out that the localized plastic deformation behavior depends on the elasticity modulus of the reinforcement particles, which leads to different macroscopic mechanical characteristics (Tomita and Lu, 2002a). Also, characterization of the polymer containing second-phase rubber particles revealed the influences of rubber particle cavitation on the micro- to macroscopic responses as well as on debonding damage at the particle surface (Tomita and Lu, 2002b). Shear band patterns in the polymer blends of polycarbonate/acrylonitrile butadiene styrene (PC/ABS) have been investigated with respect to their dependence on microstructural features such as blend composition and phase properties (Seelig and Van der Giessen, 2002).

The objective of the present study is the micromechanical modeling of the ternary polymer-based composite, which will provide the possibility of additional material selection, geometrical design, and overall synthesis. Important variables to be addressed include the elastic properties, the thickness of the interphase, and the fiber volume fraction. In the present work, in order to clarify the micro- to macromechanical behaviors of blended polymer with an interphase, we develop a computational model with constitutive equations based on the nonaffine network theory (Tomita et al., 1997). Then, the dependence of the shear band patterns and the subsequent mechanical behavior of the blended polymer on the interphase properties are clarified. In particular, we investigate the effects of the interphase on the normal stress at the fiber surface to predict the initiation of glass fiber–polymer matrix debonding damage. Thus, the effects of the elastic and geometric properties of the interphase layer on the localized plastic strain rate and normal stress at the fiber interface and the macroscopic response of the composite are clarified. Ideal characteristics of the interphase will be provided for improving the functionality of the blended polymer.

CONSTITUTIVE EQUATIONS

Constitutive equations for the glassy polymer employed in this study are given in Tomita et al. (1997) based on the nonaffine molecular chain network theory, in which, the plastic strain rate $\dot{\varepsilon}_{ij}^{p}$ is expressed as

$$\dot{\boldsymbol{\varepsilon}}_{ij}^{p} = \frac{\dot{\gamma}^{p}}{\sqrt{2}\tau}\hat{\sigma}'_{ij}, \quad \tau = \left(\hat{\sigma}'_{ij}\left(\frac{\hat{\sigma}'_{ij}}{2}\right)\right), \quad \hat{\sigma}_{ij} = \sigma_{ij} - \boldsymbol{B}_{ij} \tag{1}$$

where the direction is specified by the normalized deviatoric part of the driving stress $\hat{\boldsymbol{\sigma}}'_{ij}$, σ_{ij} is the Cauchy stress, and $\boldsymbol{B}_{ij}$ is the back-stress tensor. The shear strain rate $\dot{\gamma}^{p}$ in Equation (1) is given as (Argon, 1973)

$$\dot{\gamma}^{p} = \dot{\gamma}_0 \exp\left[\left(-\frac{As_0}{T}\right)\left\{1 - \left(\frac{\tau}{s_0}\right)^{5/6}\right\}\right], \tag{2}$$

where $\dot{\gamma}_0$ and A are constants, T is the absolute temperature, $s_0 = 0.077G/(1-\nu)$ is the athermal shear strength, G is the elastic shear modulus, ν is Poisson's ratio, and τ is the applied shear stress. The principal components of the back-stress tensor $\boldsymbol{B}_{ij}$ for the eight-chain model, which is widely used in computational simulations, are

$$\begin{aligned} B_i &= \frac{1}{3}C^{R}\sqrt{N}\frac{V_i^2 - \lambda^2}{\lambda}\mathcal{L}^{-1}\left(\frac{\lambda}{\sqrt{N}}\right), \quad \mathcal{L}(x) = \coth x - \frac{1}{x}, \\ \lambda^2 &= \left(\frac{V_1^2 + V_2^2 + V_3^2}{3}\right) \end{aligned} \tag{3}$$

where V_i is the principal plastic stretch, $\lambda_L = \sqrt{N}$ is the locking stretch, i.e., limiting stretch in tension, N is the average number of segments in a single chain, $C^{R} = nkT$ is a constant, n is the number of chains per unit volume, k is Boltzmann's constant, and $\mathcal{L}$ is the Langevin function. To accommodate the change in the entanglement situation, a nonaffine model has been proposed (Tomita et al., 1997), where the number of entangled points m becomes $m(\xi) = m_0\{-c(1-\xi)\}$. The variable ξ represents the local deformation of the polymeric material and m_0 the number of entangled points at the reference temperature $T = T_0$ and the initial state of deformation is $\xi = 1$. And c is a material constant. The final constitutive equation that relates the rate of Kirchhoff stress $\dot{S}_{ij}$ and strain rate $\dot{\varepsilon}_{kl}$ is

$$\begin{aligned} \dot{S}_{ij} &= L_{ijkl}\dot{\varepsilon}_{kl} - P'_{ij}, \quad L_{ijkl} = D^{e}_{ijkl} - F_{ijkl} \\ F_{ijkl} &= \frac{\left(\sigma_{ik}\delta_{jl} + \sigma_{il}\delta_{ik} + \sigma_{jl}\delta_{ik} + \sigma_{jk}\delta_{il}\right)}{2} \quad P'_{ij} = D^{e}_{ijkl}\frac{\dot{\gamma}^{p}}{\sqrt{2}\tau}\hat{\sigma}'_{kl} \end{aligned} \tag{4}$$

where D^{e}_{ijkl} is the elastic stiffness tensor.

COMPUTATIONAL MODEL

The viscoplastic constitutive equations presented earlier are introduced into the computational model by using the unit cell approach. This technique firstly assumes an ideal composite in which the infinitely long, unidirectionally oriented cylindrical fibers are embedded in the matrix in a periodical square arrangement displayed in Figure 1. A square fiber packing arrangement was analyzed, for which a unit cell was constructed. Because of the uniformity and symmetry of the fiber packing arrangement, all quantities averaged over a unit cell are also averages over a representative volume element (RVE) of the composite. Two unit cells were modeled, the first consisting of two phases (fiber and matrix) and the second having a third-phase interphase. Each fiber with radius r_p, consisting of an elastic material (index p) is surrounded by a coating material (interphase) of radius r_i with various material properties (index i). The matrix material (index m) is polycarbonate (PC) and assumed to undergo large deformation under applied forces. The cohesive interface condition is forced on the interfaces of the matrix and fiber, the matrix and interphase, and the interphase and fiber throughout the deformation processes, respectively, for binary and ternary systems. Considering the macroscopic strain rates ($\dot{\Gamma}_1, \dot{\Gamma}_2$) shown in Figure 1, we also discuss the effects of the macroscopic strain ratio Γ_1/Γ_2 and volume fraction of the fiber f_0 on such macroscopic deformation behavior as the average stress–strain relationship and microscopic deformation behavior of the composite.

The unit cell depicted in Figure 1 has been adopted to describe the model three-phase composites in this study. An inherent advantage of the three-phase approach used in the present study is the ability to describe quantitatively the interphase layer between the fiber and matrix. That is, the properties and thickness of the interphase layer may be chosen to reflect

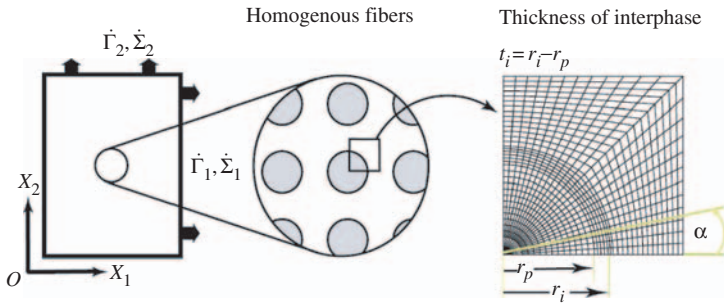

Figure 1. *Computational model.*

the integrity of fiber–matrix adhesion within the composite. For the macroscopic region, simple tension is applied with tensional strain rate $\dot{\Gamma}_2 = \dot{\varepsilon}_0 = 10^{-5}/s$, in which, the strain and stress rates are defined as $\dot{\Gamma}_1$, $\dot{\Gamma}_2$ and $\dot{\Sigma}_1$, $\dot{\Sigma}_2$, with respect to the coordinate directions X_1 and X_2. Furthermore, macroscopic equivalent stress and strain are defined as $\Sigma_e = (3\Sigma'_i\Sigma'_i/2)^{1/2}$ and $\Gamma_e = (2\Gamma'_i\Gamma'_i/3)^{1/2}$, respectively.

RESULTS AND DISCUSSION

The problems associated with the material properties of an interphase layer in a ternary polymer-based composite system were investigated by employing the computational model presented in the previous section. The properties of the glass fiber and PC matrix were held constant throughout the computational simulations unless noted otherwise. However, the properties of the interphase including mechanical properties and thickness varied. In the finite element calculations, we used the following typical material properties of glass fibers (Lauke et al., 2000) within a PC matrix (Tomita and Tanaka, 1995): $E_f = 76\,\text{GPa}$, $\nu_f = 0.22$, $E_m/s_0 = 23.7$, $\nu_m = 0.3$, $s_{ss}/s_0 = 0.79$, $h/s_0 = 5.15$, $As_0/T = 78.6$, $\alpha = 0.08$, $\dot{\gamma}_0 = 2.0 \times 10^{15}/\text{s}$, $s_0 = 97\,\text{MPa}$, $T = 296\,\text{K}$, $m_0 = 7.83 \times 10^{26}$, and $c = 0.33$.

Influences of Different Interphase Layers on the Macroscopic Response and Shear Band Pattern of Composite Material

To uncover the influence of the plastic interphase layer on the stress/strain behavior of the three-phase system under constant strain-rate loading, the analyses of different interphase glass fiber–polymer composites were performed. In this study, the interphases consisted of two different types of polymers with Poisson's ratios continuously changing from 0.25 to 0.499. The mechanical properties of four interphases that have been selected for illustration are given in Table 1. The results shown in Figures 2–4 were obtained under the following conditions: the volume fraction of the fiber $f_0 = 20\%$, interphase thickness to fiber radius $t_i/r_p = 0.2$, and different macroscopic strain ratios (Γ_1/Γ_2).

Table 1. Mechanical properties of interphases.

Material	E_i (GPa)	ν_i	s_{ss}/s_0	h/s_0	C_R
Thermoplastic polypropylene-I (TPP-I)	0.5	0.3	0.92	9.28	12.8
Thermoplastic polypropylene-II (TPP-II)	0.5	0.49	–	–	–
Thermoplastic polyurethane-I (TPU-I)	0.33	0.3	–	–	–
Thermoplastic polyurethane-II (TPU-II)	0.33	0.49	–	–	–

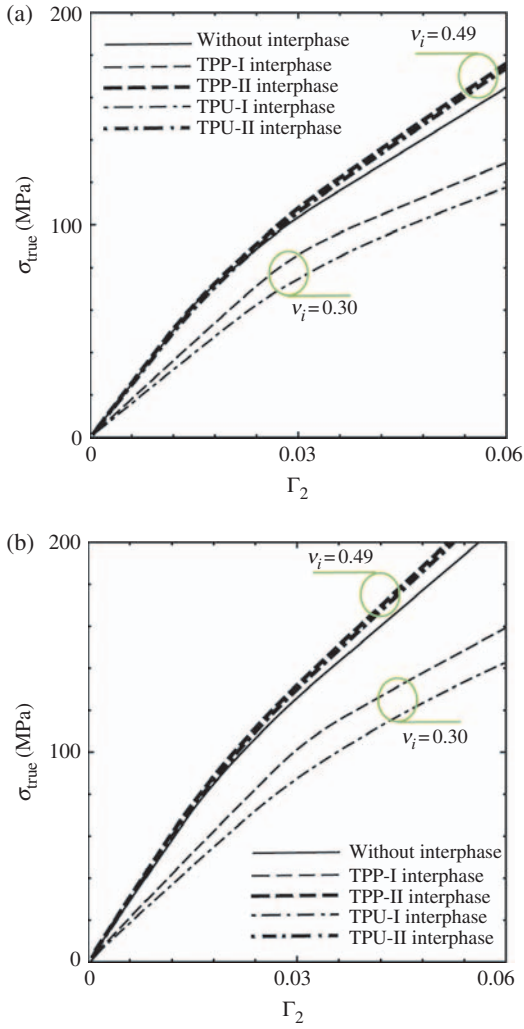

Figure 2. *True stress vs true strain for $f_0 = 20\%$, $t_i/r_p = 0.2$: (a) $\Gamma_1/\Gamma_2 = 0.0$ and (b) $\Gamma_1/\Gamma_2 = 0.4$.*

Figure 2 illustrates the true stress versus true strain relations for a unit cell with different interphases. For the purpose of comparison, the two-phase model without an interphase is also presented. The responses under different macroscopic strain ratio conditions exhibit qualitatively the same characteristics as the two shown in Figure 2. Increasing the macroscopic strain ratio results in an increase of the magnitude of the macroscopic

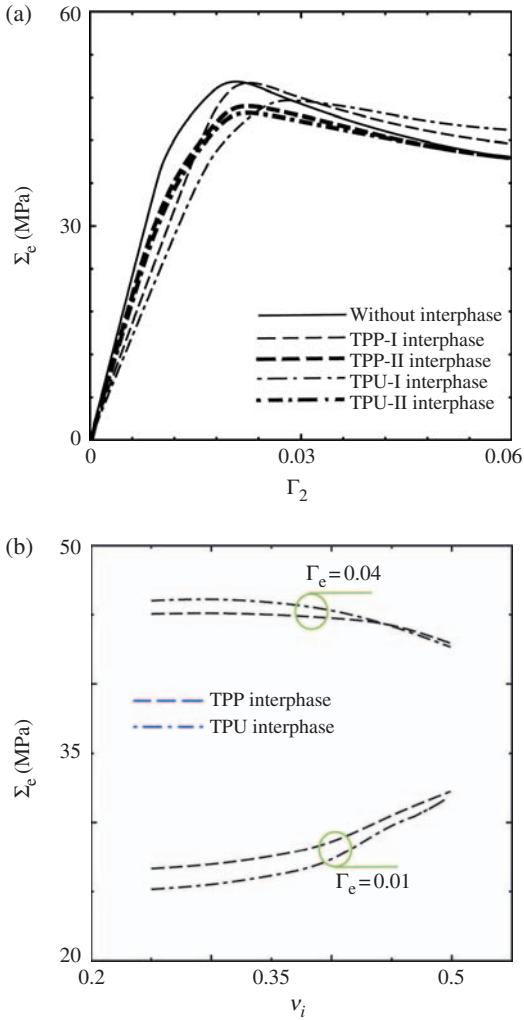

Figure 3. *(a) Macroscopic equivalent stress vs equivalent strain and (b) macroscopic equivalent stress vs interphase Poisson's ratio of two different interphase stiffness for* $f_0 = 20\%$, $t_i/r_p = 0.2$ *and* $\Gamma_1/\Gamma_2 = 0.0$.

stresses in different models, whereas the influence of interphase properties is independent of the change of the macroscopic strain ratio. The true stress of unit cell seems to be considerably influenced by the interphase elastic properties. In a previous study (Esmaeili and Tomita, 2006), we found that the incorporation of a polymeric interphase with a stiffness lower than that of the matrix results in a reduction of the macroscopic stress of

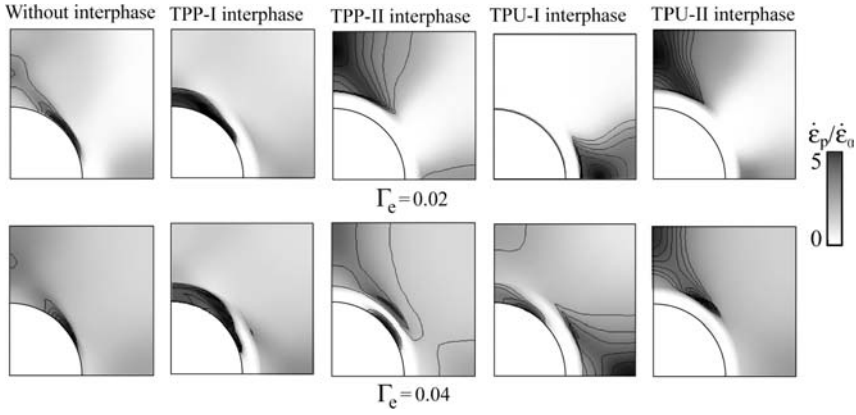

Figure 4. *Plastic strain rate distribution for $f_0 = 20\%$, $t_i/r_p = 0.2$, and $\Gamma_1/\Gamma_2 = 0.0$.*

the composite. While a rather soft interphase causes a greater reduction in the true stress when Poisson's ratio of the interphase is low, the effect of interphase stiffness diminishes with increasing interphase Poisson's ratio. Indeed, the true stress seems insensitive to the change of the interphase stiffness for a very high Poisson's ratio of the interphase.

Macroscopic equivalent stresses versus equivalent strain of the unit cells are shown in Figure 3(a), and the sensitivity of this value to the interphase Poisson's ratio is illustrated in Figure 3(b). Unlike the true stress, the macroscopic equivalent stress does not seem to be greatly influenced by the interphase layer. For a composite with a softer polymeric interphase, thermoplastic polyurethane (TPU), the suppression of the elasticity modulus is observed in both Figures 3(a) and (b) particularly for a lower Poisson's ratio of the interphase ($\nu_i = 0.3$). Increasing the interphase Poisson's ratio intensifies the rate of change of the macroscopic equivalent stress, as seen in Figure 3(b); however, it suppresses the effect of interphase stiffness. In other words, the macroscopic equivalent stresses with different interphase stiffnesses tend to converge at an interphase Poisson's ratio of about $\nu_i = 0.5$. In fact, with a higher Poisson's ratio of the interphase ($\nu_i = 0.49$), the macroscopic deformation resistance seems almost identical to the change of the interphase modulus of elasticity due to the liquid-like deformation of interphases with high Poisson's ratio.

For both TPU and thermoplastic polypropylene (TPP) interphase, a considerable reduction of macroscopic yield upon increasing the interphase Poisson's ratio is of interest. Points of low yield observed for the cases of TPU-II and TPP-II, are a consequence of an increased composite modulus due to the high Poisson's ratios of the interphase. It is also notable that after yielding, deformation resistance of the composite

increases slightly in the plastic region in the cases of low Poisson's ratios of the interphase due to increased macroscopic equivalent stress of the composite. Moreover, the maximum deformation resistance of the unit cell is slightly enhanced in the plastic region as the stiffness of the polymer interphase decreases. On the other hand, when the interphase is softer than the matrix, the three-phase composite becomes substantially softer than the two-phase system. However, a hard interphase does not contribute to the decrease in stiffness of the three-phase system.

The plastic strain rate distributions in two different deformation stages are shown in Figure 4. As illustrated, shear bands are significantly influenced by both the interphase modulus of elasticity and Poisson's ratio. With a lower interphase Poisson's ratio, a high-plastic-strain-rate region appears at the pole of the fiber and within the interphase (TPP-I interphase in Figure 4). However, with the TPU-I interphase, the high-plastic-strain-rate region appears at the equator of the fiber inside the matrix, which is comparable to the effect of soft inclusion in the two-phase model (Tanaka et al., 2000) and is associated with a marked reduction in the true stress and macroscopic equivalent stress of the composite, as already described in Figures 2 and 3(a). For both TPU-II and TPP-II interphases, the high-plastic-strain-rate region moves toward the pole within the matrix and is distributed in a more widely spread area as a result of the high Poisson's ratio.

The different types of propagation of the shear band in the deformation stages cause differences in the macroscopic yield points and in the macroscopic deformation behavior as indicated previously in Figures 2 and 3. On the other hand, the main characteristic features of shear band developments are almost identical to those in the cases of very high Poisson's ratio of the interphase ($\nu_i = 0.49$ cases in Figure 4). In fact, with the increase of interphase Poisson's ratio, the shear band moves toward the pole and propagates within the matrix (Figure 4), which expands plastic strain rate distribution in the polymer, and is attributable to the reduction of the macroscopic yield stress as is observed in Figure 3(a).

The aforementioned result clarifies that the introduction of an interphase effectively changes the onset and propagation of the shear band in the polymer, which subsequently changes the magnitude of the macroscopic stress of the composite. A proper combination of the elastic properties of the interphase is required to keep the deformation resistance of the composite unchanged. A plastic interphase with stiffness lower than that of the matrix causes a reduction in macroscopic deformation resistance. While increasing the interphase stiffness has a positive effect on the increase of macroscopic yielding, increasing the interphase Poisson's ratio adversely reduces it. The incorporation of an interphase with a stiffness lower than that of the

matrix results in a reduction of the macroscopic stress of the composite. However, if the interphase is nearly incompressible ($\nu_i \cong 0.49$), this is no longer true.

Prediction of Initiation of Debonding Damage at Fiber Surface

The initiation of debonding damage can be predicted using the finite element model. To simulate the fiber–matrix debonding process, a tensile debonding criterion may be applied to the interface elements, because the interface is the most critical region in which fiber–matrix debonding occurs. This failure is assumed to occur in the interface element when the microscopic tensile stresses normal to the interfaces exceed a critical stress. As the glass fibers are relatively stiff compared with the matrix, the radial stress corresponds to the normal stress at the interface. If the fiber is soft relative to the matrix, it will deform into an elliptical shape under tensile load, and normal stress at the interface will deviate from the radial stress. This must also be considered if the normal stress at the interphase/matrix interface must be determined, because the interphase deforms into an ellipse. In this study, since the influence of the interphase on the debonding behavior of the composite is considered, a cohesive interface condition is forced on the interfaces, and the stress normal to an interface is assumed to be responsible for the initiation of debonding. The normal stress is defined as

$$\sigma_n = \frac{1}{2(\sigma_{11}+\sigma_{22})} + \frac{1}{2(\sigma_{11}-\sigma_{22})}\cos(2\alpha) + \sigma_{12}\sin(2\alpha) \tag{5}$$

where angle α is shown in Figure 1.

Based on the preceding description of the initiation of debonding damage and considering the results in the previous section, we here set out to investigate the normal stress and plastic strain rate distributions on the fiber surface. Figure 5 shows the maximum normal stress on the fiber surface, which considerably decreases when TPP-I or TPU-I interphase is used. However, in contrast with models without an interphase, the incorporation of the TPP-II or TPU-II interphases causes minimal change in the maximum normal stress, as Figure 5(a) reveals. As can be observed in Figure 5(b), the effect of interphase stiffness on the maximum normal stress is suppressed by increasing Poisson's ratio of the interphase. In a previous study (Esmaeili and Tomita, 2006), we considered $\nu_i = 0.3$ and different interphase stiffnesses, and concluded that a modulus lower than that of the matrix results in a reduction of most critical stress concentrations in the neighborhood of the inclusion. However, this result suggests that with an

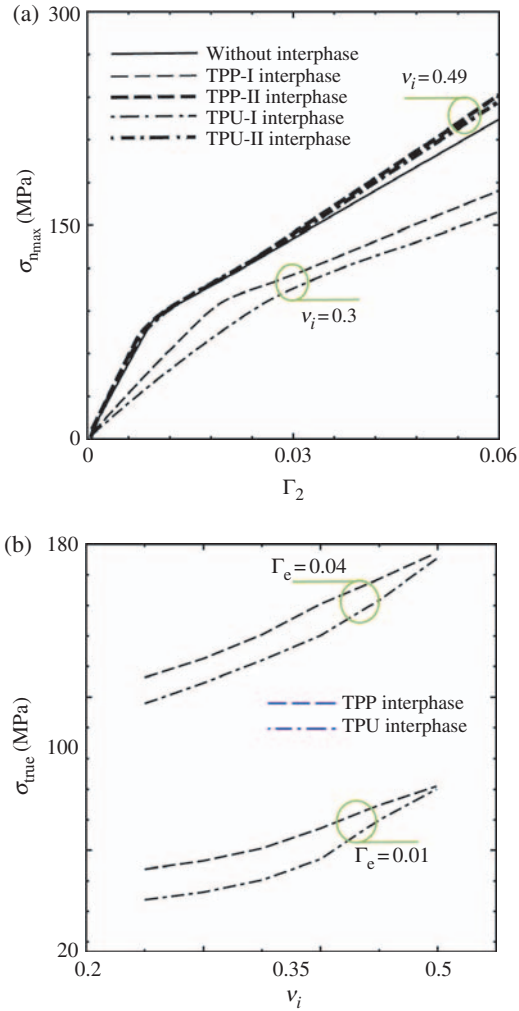

Figure 5. *(a) Maximum normal stress vs equivalent strain and (b) maximum normal stress vs interphase Poisson's ratio of two different interphase stiffness for* $f_0 = 20\%$, $t_i/r_p = 0.2$ *and* $\Gamma_1/\Gamma_2 = 0.0$.

interphase material having a high Poisson's ratio, this conclusion would not be valid, and emphasizes the role of Poisson's ratio even in a plastically deforming interphase. A similar tendency can also be observed in the case of an elastic interphase (Esmaeili et al., 2004) where, due to a liquid-like deformation of interphases with high Poisson's ratio ($\nu_i \cong 0.49$), local stresses become almost identical to the change of the interphase stiffness.

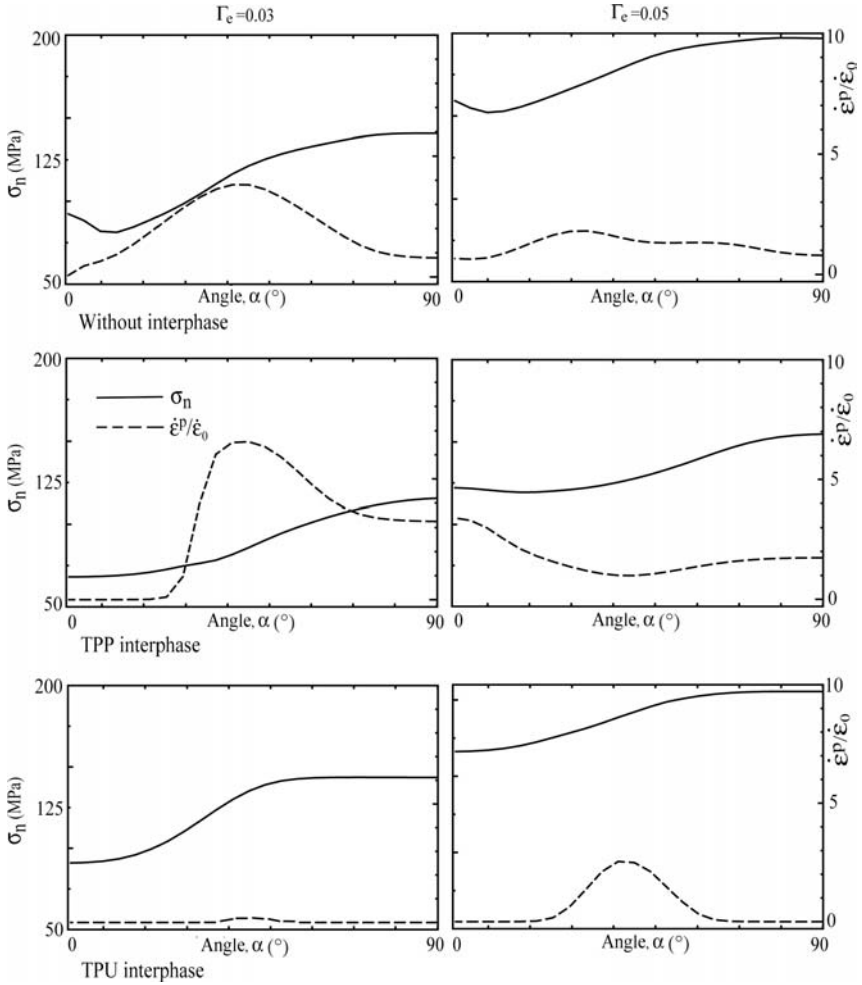

Figure 6. *Normal stress and plastic strain rate distribution on the fiber surface for $f_0 = 20\%$, $t_i/r_p = 0.2$ and $\Gamma_1/\Gamma_2 = 0.0$: (a) $\Gamma_e = 0.03$ and (b) $\Gamma_e = 0.05$.*

Figure 6 depicts the normal stress distribution along the fiber surface at two different deformation levels of $\Gamma_e = 0.03$ and 0.05. To clearly show the relationship between the shear band and the point with a high normal stress, the equivalent plastic strain rate distributions are also shown in the same figure. The distribution of the plastic strain rate at the interface is as previously shown in Figure 4. The plastic strain rate is low on the fiber surface in the case of the TPP-II interphase similar to the model without an interphase, whereas, in the case of the TPP-I interphase a high plastic strain

rate region, which appears around the fiber, suppresses the normal stress at the interface. Under the assumption that only the stresses normal to an interface are responsible for the initiation of debonding, it is suggested that the use of a softer polymeric interphase with properly selected Poisson's ratio will reduce the probability of debonding. It is also interesting to note that the normal stress changes are rather smooth in the presence of an interphase. Thus, the possibility of moderization of the normal stresses around the fiber arises with the introduction of a proper interphase layer.

The location of the maximum normal stress and consequent initiation of debonding is also be slightly affected by interphase properties. The location of the maximum normal stress at the fiber surface in a model without an interphase is nearly at the pole, which is in agreement with results in the literature (Lauke et al., 2000; Lee et al., 2000), however it moves toward the pole with the TPP-I interphase. The reason for the shift in the position of the maximum normal stress toward the pole lies in the nonlinear behavior of the interphase material. The total strain around the inclusion is superimposed by elastic and plastic contributions. Plastic flow does not first occur at the fiber/interphase interface but does so within the TPP-I interphase, as previously described in Figures 4 and 6, respectively. This may cause local unloading and increases of stresses in other regions.

A clearer indication of the normal stress and plastic strain rate in each constituent is given in Figure 7, in which the normal stress and plastic strain rate are shown in radial distance at the pole where the maximum normal stress of the fiber surface occurs. As Figure 7 suggests, the normal stresses and plastic strain rates within the fiber, interphase, and matrix are significantly influenced by the elastic properties of the interphase. A low stiffness of the interphase has the effect of decreasing the average stress and consequently the normal stress of the composite, whereas a high Poisson's ratio of the interphase increases the normal stress in all phases, also as a result of increased average stress. In both stages of deformation, high-plastic-strain-rate is concentrated inside the TPP-I interphase, as previously explained in Figure 4. However, the amount of normal stress reduction seems to be the same in all three phases, regardless of the considerable differences in the magnitudes of the plastic strain rate.

The results of the analysis of a polymeric interphase (TPP-I) are of special interest. As described in Figure 3, this type of interphase was found to cause a moderate reduction of the macroscopic deformation resistance of the unit cell. Furthermore, according to Figures 5–7, it considerably reduces the stress concentration in the neighborhood of the fiber. As Young's modulus of this interphase is well below those of the fiber and the matrix, the interphase deforms much more easily than the matrix. Since the more deformable and soft interphase is coated directly to the filler instead of the

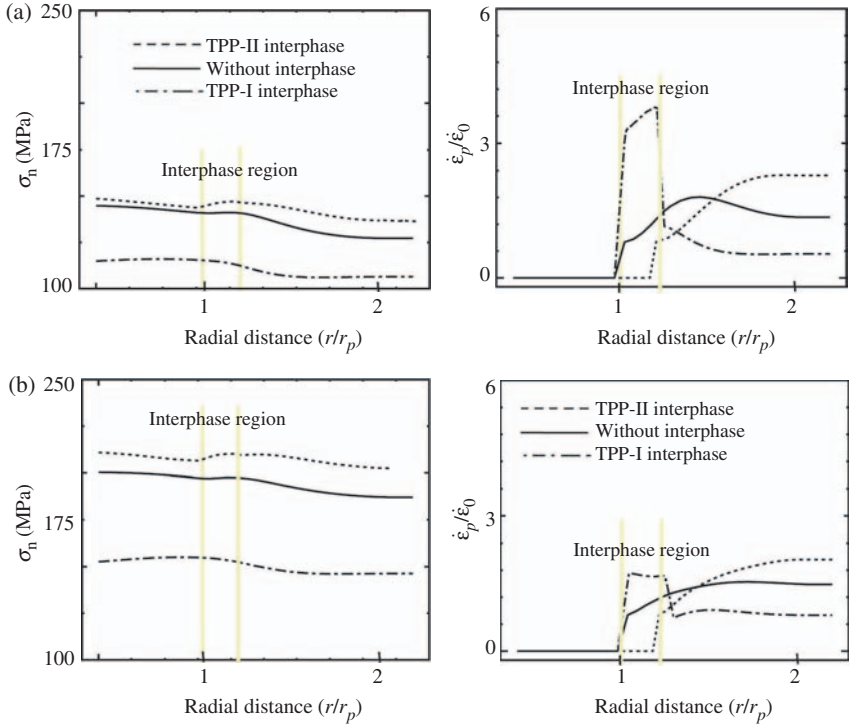

Figure 7. *Normal stress and plastic strain rate distribution within fiber, interphase and matrix at pole of fiber for* $f_0 = 20\%$, $t_i/r_p = 0.2$ *and* $\Gamma_1/\Gamma_2 = 0.0$.

matrix, there is a reduction in stresses around the fibers induced by deformation, in compatibility with the composite. Moreover, Poisson's ratio less than 0.49 do not contribute to the increase of the normal stresses. Thus, the three-phase composite filled with glass fibers coated with a suitable polymeric interphase has a lower normal stress at the interfaces than that in the two-phase composite with the same glass fibers. Referring to Figures 2–6, the current results suggest that the introduction of a specific soft interphase realizes a high deformation resistance, accompanied by a reduction in stress concentration in the neighborhood of the fiber that suppresses the probability of debonding.

Effect of Interphase Thickness and Fiber Volume Fraction on the Initiation of Debonding Damage

In the previous sections, it was clarified that the micro- to macroscopic responses of the composite are strongly influenced by Young's modulus

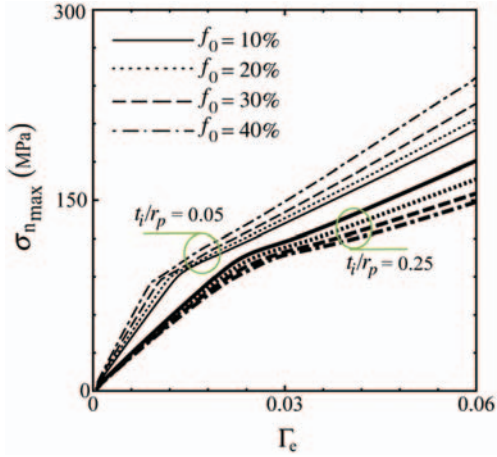

Figure 8. *Maximum normal stress on the fiber surface vs macroscopic equivalent strain for* $\Gamma_1/\Gamma_2 = 0.0$.

and Poisson's ratio of the interphase. Specifically, a polymeric interphase (TPP-I) was found, in most cases, to have a beneficial effect on the reduction of the normal stress on the fiber surface, which suppresses the initiation of debonding without causing a marked reduction in the macroscopic deformation resistance of the unit cell. Here, we investigate the effect of the interphase thickness as well as fiber volume fraction on the initiation of debonding damage between the glass fiber and the PC matrix.

The maximum normal stress for different fiber volume fractions and interphase thicknesses are shown in Figures 8 and 9, respectively. As Young's modulus of the TPP-I interphase is much less than those of the matrix and the fiber, a rather thick interphase markedly decreases the maximum normal stress on the fiber surface. However, while increasing the fiber volume fraction results in an increase of the maximum normal stress on the fiber surface when the interphase is thin ($t_i/r_p = 0.05$), it causes diverse effects in the presence of a thick interphase ($t_i/r_p = 0.25$). Indeed, as depicted in Figure 9, the reduction rate of the maximum normal stress depends on the fiber volume fraction and interphase thickness in any deformation stage. This rate increases with increasing fiber volume fraction; however, the effect of the fiber volume fraction on the normal stress disappears at a specific interphase thickness.

It has already been found (Esmaeili and Tomita, 2006) that the effect of a soft interphase on the maximum normal stress is distinct from that of a hard interphase. With the soft interphase, the maximum normal stress decreases

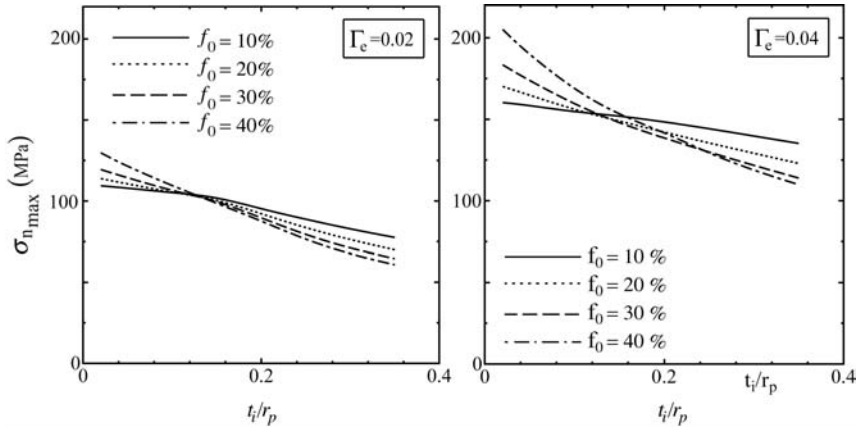

Figure 9. *Maximum normal stress on the fiber surface vs interphase thickness for* $\Gamma_1/\Gamma_2 = 0.0$.

with the increase of interphase thickness, while it increases with interphase thickness in the case of a hard interphase.

These results again emphasize that a specific soft interphase, i.e., TPP-I interphase, that has a yield stress lower than that of the matrix, greatly reduces the probability of debonding at the fiber surface. On the contrary, if the interphase is stiffer than the matrix, increasing its thickness will further promote the initiation of debonding. Figure 10 shows the normal stress distribution along the interfaces of the matrix and the fiber for different interphase thicknesses at four deformation stages. Regardless of the arrival of strain localization zones, which were previously shown in Figures 4 and 6, the distribution patterns of normal stress with interphases are almost unchanged. The present interphase (TPP-I) favorably reduces the magnitude of the normal stress on the fiber surface. On the other hand, the relative difference with respect to that of the two-phase composite changes with the deformation.

The interphase thickness, in fact, enhances the contribution of the effect of material parameters on the mechanical characteristics of the composites. However, in order to achieve advantageous or the desired composite characteristics, the influence of other parameters, such as fiber volume fraction, should also be taken into account, because, although increasing the fiber volume fraction results in an increase of the maximum normal stress in the presence of a thin interphase, it causes a diverse effects with a thicker interphase. As a consequence, it is suggested that, when we design the interphase, particularly one coated onto the fiber or particles, the appropriate combination of the interphase thickness and fiber volume

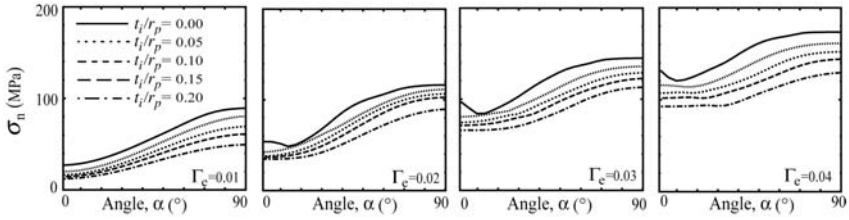

Figure 10. *Normal stress distribution along the interface of the matrix and fiber for $f_0 = 20\%$ and $\Gamma_1/\Gamma_2 = 0.0$.*

fraction should be determined in order to achieve the desired behavior of the composite.

CONCLUSIONS

A computational method employing a plane-strain unit cell has been developed in order to clarify the effects of interphase properties on the fiber-reinforced polymer. The elasto-plastic behaviors of the composite have been confirmed to be influenced by the interphase properties, which were successfully characterized using two polymeric interphases with continuously changing Poisson's ratios from 0.25 to 0.49. The simulations were designed particularly toward describing the debonding behavior of a composite, in which polymer is incorporated as the interphase that bond glass fibers to the polymeric matrix. Under the assumption of a cohesive interface, the prediction of the initiation of fiber–matrix debonding was considered, by investigating the normal stress at the fiber surface as the governing parameter in the initiation of debonding. Moreover, we evaluated the effects of the macroscopic strain ratio, the interphase properties, and the fiber volume fraction on macroscopic characteristics, such as deformation resistance and yield stress, on microscopic characteristics, such as the shear band pattern, and normal stress on the fiber surface and within all phases. The results are summarized as follows:

1. A soft interphase causes a marked reduction in the macroscopic stress in the case of an interphase with low Poisson's ratio; however, the effect of the interphase stiffness diminishes with increasing interphase Poisson's ratio. Increasing the interphase Poisson's ratio expands the plastic strain rate distribution, which is attributable to the reduction of the macroscopic yield stress.
2. The influence of the interphase stiffness on the maximum normal stress is suppressed by increasing the interphase Poisson's ratio although the rate of change of the normal stress increases. In fact, due to the liquid-like

deformation of interphases with high Poisson's ratios ($\nu_i \cong 0.49$), local stresses become almost identical to the change of the interphase stiffness.
3. Plastic flow first occurs not at the fiber/interphase interface but within the soft TPP-I interphase, which may cause local unloading and increased stresses in other regions. Also, the high-plastic-strain-rate region, which appears around the fiber, suppresses the normal stress at the interface.
4. While an interphase stiffness lower than that of the matrix has the effect of decreasing the average stress of the unit cell and consequently the normal stress inside each constituent of the composite, a high Poisson's ratio of the interphase increases the normal stress in all phases as a result of the raised average stress.
5. While increasing the interphase thickness markedly reduces the maximum normal stress on the fiber surface, a high fiber volume fraction increases it. The rate of change of the normal stress depends on both fiber volume fraction and interphase thickness. The effect of the fiber volume fraction on the normal stress disappears at a specific interphase thickness.

ACKNOWLEDGMENTS

Financial support and Scholarship from the Ministry of Education, Science, Sports and Culture of Japan are gratefully acknowledged.

REFERENCES

Argon, A.S. (1973). A Theory of Low-Temperature Plastic Deformation of Glassy Polymers, *Phil. Mag*., **28–39**: 839–865.

Arruda, E.M. and Boyce, M.S. (1993). A Three-dimensional Constitutive Model for Large Stretch Behavior of Rubber Materials, *J. Mech. Phys. Solids*, **41**: 389–412.

Eirich, F.R. (1984). Some Mechanical and Molecular Aspects of the Performance of Composites, *Appl. Polym. Symp*., **39**: 93–102.

Esmaeili, N. and Tomita, Y. (2006). Micro- to Macroscopic Responses of a Glass Particle-Blended Polymer in the Presence of an Interphase Layer, *Int. J. Mech. Sci*., **48**: 1186–1195.

Esmaeili, N., Lu, W. and Tomita, Y. (2004). Effects of Interphase Properties on the Mechanical Behavior of Trinary Polymer-Based Composites, In: Yao, Z.H., Yuan, M.W. and Zhong, W.X. (eds), *The 6th World Congress on Computational Mechanics in Conjubction with the Second Asian-Pacific Congress on Computational Mechanics* (Compact Disc).

Fan, J.P., Tsui, C.P. and Tang, C.Y. (2004). Modeling of the Mechanical Behavior of HA/PEEK Biocomposite Under Quasi-Static Tensile Load, *Mater. Sci. Eng*., **382**: 341–350.

Johnson, A.C., Hayes, S.A. and Jones, F.R. (2005). An Improved Model Including Plasticity for the Prediction of the Stress in Fibers with an Interface/Interphase Region Composites, *Composites Part A: Appl. Sci. Manufacturing*, **36**: 263–271.

Kardos, J.L. (1985). In: Ishida and Kumar (eds), *Molecular Characterization of Composite Interfaces*, pp. 1–11, Plenum, New York.

Lauke, B., Schuller, T. and Beckert, W. (2000). Calculation of Adhesion Stretch at the Interface of a Coated Particle Embedded Within Matrix Under Multiaxial Load, *Compos. Mater. Sci.*, **18**: 362–380.

Lee, S.T., Chiang, H.C., Lin, C.T., Huang, H.M. and Dong, D.R. (2000). Finite Element Analysis of Thermo-debonding Mechanism in Dental Composites, *Biomaterials*, **21**: 1315–1326.

Li, G.C., Ling, X.W. and Shen, H. (2000). On the Mechanism of Void Growth and the Effect of Straining Mode in Ductile Materials, *Int. J. Plast.*, **16**: 39–51.

Llorca, J., Elices, M. and Termonia, Y. (2000). Elastic Properties of Sphere-reinforced Composites with a Meshophase, *Acta Material*, **48**: 4589–4597.

Mai, K., Mäder, E. and Mühle, M. (1998). Interphase Characterization in Composites with New Non-Destructive Methods, *Composites*, **29A**: 1111–1119.

Pijnenburg, K.G.W. and Van der Giessen, E. (2001). Macroscopic Yield in Cavitated Polycarbonate, *Int. J. Solids Structs.*, **38**: 3575–3598.

Pukánszky, B. (1990). Influence of Interface Interaction on the Ultimate Tensile Properties of Polymer Composites, *Composites*, **25**: 255–262.

Seelig, T.H. and Van der Giessen, E. (2002). Localized Plastic Deformation in Ternary Polymer Blends, *Int. J. Solids Structs.*, **39**: 3505–3522.

Tanaka, S., Tomita, Y. and Lu, W. (2000). Computational Simulation of Deformation Behavior of Glassy Polymer With Cylindrical Inclusions Under Tension, *Trans. JSME*, **66A**: 36–45 (in Japanese).

Tomita, Y. and Lu, W. (2002a). Characterization of Micro- to Macroscopic Response of Polymers Containing Second-Phase Particles Under Macroscopically Uniform Deformation, *Int. J. Solids Structs.*, **39**: 3409–3428.

Tomita, Y. and Lu, W. (2002b). Computational Characterization of Micro- to Macroscopic Response and Damage of Polymers Containing Second-Phase Particles, *Int. J. Damage Mech.*, **11**: 129–149.

Tomita, Y. and Tanaka, S. (1995). Prediction of Deformation Behavior of Glassy Polymers Based on Molecular Chain Network Model, *Int. J. Solids Structs.*, **32**: 3423–3434.

Tomita, Y., Adachi, T. and Tanaka, S. (1997). Modeling and Application of Constitutive Equation for Glassy Polymer Based on Nonaffine Network Theory, *Eur. J. Mech. -A/Solids*, **16**: 745–755.